On the relationships between local vortex identification schemes

By PINAKI CHAKRABORTY, S. BALACHANDAR
AND RONALD J. ADRIAN

Department of Theoretical and Applied Mechanics, University of Illinois
at Urbana-Champaign, Urbana, IL 61801, USA

We analyse the currently popular vortex identification criteria that are based on point-wise analysis of the velocity gradient tensor. A new measure of spiralling compactness of material orbits in vortices is introduced and using this measure a new local vortex identification criterion and requirements for a vortex core are proposed. The inter-relationships between the different criteria are explored analytically and in a few flow examples, using both zero and non-zero thresholds for the identification parameter. These inter-relationships provide a new interpretation of the various criteria in terms of the local flow kinematics. A canonical turbulent flow example is studied, and it is observed that all the criteria, given the proposed usage of threshold, result in remarkably similar looking vortical structures. A unified interpretation based on local flow kinematics is offered for when similarity or differences can be expected in the vortical structures educed using the different criteria.

1. Introduction

Vortices are often viewed as "the sinews and muscles of turbulence" (Küchermann 1965) and yet their identification is hindered by the lack of an accepted mathematical definition of a 'vortex' (our usage of the term 'vortex' refers to a 'vortex core', see Jeong & Hussain 1995). It may seem surprising that in a long-studied field such as fluid mechanics a fundamental question like this still has no clear answer. As noted by Chong, Perry & Cantwell (1990) "...it is unlikely that any definition of a vortex will win universal acceptance". Indeed, no single definition of a vortex is currently universally accepted, despite the fact that fluid dynamicists continue to think in terms of vortices.

The characteristic shapes of vortical structures in turbulence are a question of long-standing interest (for some reviews on this topic refer to Cantwell 1981; Hussain 1986; Robinson 1991). Through study of the velocity gradient tensor, regions of vorticity in the form of filaments, sheets, and blobs have been identified. Vortex filaments play an important role in the overall turbulence dynamics: vortex 'worms' in isotropic turbulence (Jiménez *et al.* 1993), vortex 'braids' in turbulent shear layers (Rogers & Moser 1994), quasi-streamwise vortices (Robinson 1991; Brook & Hanratty 1993), and 'hairpin' vortices in wall turbulence (Head & Bandyopadhyay 1981; Smith *et al.* 1991; Adrian, Meinhart & Tomkins 2000) are important examples of coherent structures that approximate vortex filaments.

The term 'vortex filament' connotes a long, thin vortical structure, as opposed to a three-dimensional blob, or a two-dimensional vortex sheet, or a field of constant

vorticity such as a uniform shear flow. Likewise, it implies a finite-diameter core in which vorticity is concentrated, and hence the non-uniform spatial distribution of vorticity is an essential element in the definition. In ideal fluids the existence of a sharp boundary between rotational and irrotational fluid results in an unequivocal definition of a vortex filament (Saffman 1992). In real fluids, however, the diffusion of vorticity by viscosity prohibits the possibility of such a crisp definition. The diffusion by viscosity, coupled with the interaction of vorticity distribution with strain field, makes the problem of identifying vortex filaments in real fluids quite complicated.

The vortex filament is an attractive fluid dynamic concept for several reasons. First and foremost, it allows simple understanding of a large part of the entire flow using the law of Biot-Savart. To be able to apply the law of Biot-Savart or higher-order approximations (cf. Moore & Saffman 1972) it is necessary for the core diameter of a finite filament to be small compared to the radius of curvature of the filament. Since the filament itself occupies a rather small volume, the Biot-Savart law effects a type of data compression, making the entire flow understandable in terms of the vortex-induced flow and the dynamics of the filament.

It appears that common usage of the term 'vortex core' often implies a filamentary geometry. Commonly used intuitive definitions of a vortex also contain the essential characteristics of the flow induced by a vortex filament. For example, Lugt (1979) requires that a vortex should have a multitude of material particles rotating around a common centre; Robinson (1991) states "A vortex exists when instantaneous streamlines mapped onto a plane normal to the vortex core exhibit a roughly circular or spiral pattern, when viewed from a reference frame moving with the centre of the vortex core".

Local or point-wise methods of vortex identification define a function that can be evaluated point-by-point and then classify each point as being inside or outside a vortex according to a criterion based on the point values. Most local vortex identification criteria are based on the kinematics implied by the velocity gradient tensor, ∇v, thereby making them Galilean invariant. The most popularly used local criteria are: Q (Hunt, Wray & Moin 1988), λ_2 (Jeong & Hussain 1995), Δ (Chong *et al.* 1990), and λ_{ci} (Zhou *et al.* 1999). The next section gives an overview of these criteria. All the above criteria are concerned with detecting vortex filaments. In fact, one of the chief virtues of these detection methods is that they discriminate against vortex sheets, rendering the vortex filaments more visible in complex vorticity fields. Although these criteria are developed for isolated vortex filaments, they are frequently applied to complex flows with interacting vortices. The objective of identifying the most intense structures usually justifies this application; however, the educed structure should be interpreted with care. The educed vortex structure obtained from the usage of these kinematic criteria can be used as a basis for formulating dynamic models of flow evolution (for example refer to Perry & Marusic 1995; Marusic 2001).

In this paper we consider vortex identification by restricting attention to the special case of a vortex filament. Non-filamentary vorticity distributions also play an important role in the dynamics of many flows, but are not a subject of the present investigation. The local criteria discussed here can be modified to identify such non-filamentary vorticity regions (for example see Tanaka & Kida 1993; Horiuti 2001). This paper describes an extension of the swirling strength criterion described by Zhou *et al.* (1999) by introducing a two-parameter system for vortex identification. These parameters measure the swirling strength and spiralling compactness of the local streamline geometry. A survey of literature yields contradictory results regarding the comparison of vortex structure educed using the different local criteria. For example,

Jeong & Hussain (1995) observe significant differences in various flow examples, whereas Dubief & Delcayre (2000) see remarkably similar looking structures for many turbulent flows. We use our two-parameter system to analytically relate the different schemes and form a physical basis for explaining these observations. This allows us to formulate a unified interpretation by reconciling the different observations using the two-parameter system and understand the nature of the similarity or differences, as opposed to a simple comparison. The relationship with the various schemes in terms of the two kinematic parameters provides a new interpretation of the different criteria in terms of the local kinematics of the flow. The intense structures in many turbulent flows are seen to be approximately locally two-dimensional with limited radial motion, based on which we propose a simple 'equivalent threshold' that results in remarkably similar looking vortical structures extracted by the different criteria.

2. Background of vortex identification schemes

In this section we provide an overview of popular local schemes and one non-local scheme for vortex identification. The reader is referred to Jeong & Hussain (1995) for a discussion on the inadequacies of common intuitive measures of detecting vortices: local pressure minima, closed or spiralling streamlines and pathlines, and iso-vorticity surfaces.

2.1. *Local approaches based on velocity gradient tensor*

We briefly discuss Galilean invariant vortex identification techniques based on local analysis of the velocity gradient tensor, ∇v.

2.1.1. *Q criterion*

The Q criterion (Hunt *et al.* 1988) identifies vortices as flow regions with positive second invariant of ∇v, i.e. $Q > 0$. Additionally, the pressure in the eddy region is required to be lower than the ambient pressure. The second invariant, Q (defined as $Q = ((\nabla \cdot v)^2 - \mathrm{tr}(\nabla v^2))/2)$, for an incompressible flow ($\nabla \cdot v = 0$) can be written as

$$Q = \tfrac{1}{2}(\|\boldsymbol{\Omega}\|^2 - \|\boldsymbol{S}\|^2), \qquad (2.1)$$

where $\|\boldsymbol{\Omega}\| = \mathrm{tr}[\boldsymbol{\Omega}\boldsymbol{\Omega}^t]^{1/2}$ and $\|\boldsymbol{S}\| = \mathrm{tr}[\boldsymbol{S}\boldsymbol{S}^t]^{1/2}$; $\boldsymbol{S}$ and $\boldsymbol{\Omega}$ are the symmetric and anti-symmetric components of ∇v defined as $\boldsymbol{S} = \tfrac{1}{2}(\nabla v + (\nabla v)^t)$ and $\boldsymbol{\Omega} = \tfrac{1}{2}(\nabla v - (\nabla v)^t)$ respectively. Hence, in an incompressible flow Q is a local measure of the excess rotation rate relative to the strain rate.

Note that $Q > 0$ does not guarantee the existence of a pressure minimum inside the region identified by it (Jeong & Hussain 1995). In most cases, however, the pressure condition is subsumed by $Q > 0$ (Jeong & Hussain 1995; Dubief & Delcayre 2000, refer to their discussion on a thin low-pressure tube). In this paper we use the Q criterion without the additional pressure condition.

2.1.2. λ_2 *criterion*

The λ_2 criterion (Jeong & Hussain 1995) is formulated based on the observation that the concept of a local pressure minimum in a plane fails to identify vortices under strong unsteady and viscous effects. By neglecting these unsteady and viscous effects, the symmetric part of the gradient of the incompressible Navier–Stokes equation can be expressed as

$$\boldsymbol{S}^2 + \boldsymbol{\Omega}^2 = -\frac{1}{\rho}\nabla(\nabla p), \qquad (2.2)$$

where p is the pressure and equation (2.2) is a representation of the pressure Hessian $((\nabla(\nabla p))_{ij} = \partial^2 p / \partial x_i \partial x_j)$. To capture the region of local pressure minimum in a plane, Jeong & Hussain (1995) define the vortex core as a connected region with two positive eigenvalues of the pressure Hessian. We comment on this requirement later in this section. If the eigenvalues of the symmetric tensor $\mathbf{S}^2 + \mathbf{\Omega}^2$ are ordered as $\lambda_1 \geqslant \lambda_2 \geqslant \lambda_3$, this definition is equivalent to the requirement that $\lambda_2 < 0$ at every point inside the vortex core. The eigenvalues of $\mathbf{S}^2 + \mathbf{\Omega}^2$ and Q are related by (Jeong & Hussain 1995)

$$Q = -\tfrac{1}{2}\mathrm{tr}(\mathbf{S}^2 + \mathbf{\Omega}^2) = -\tfrac{1}{2}(\lambda_1 + \lambda_2 + \lambda_3). \tag{2.3}$$

It can be shown that while the Q criterion measures the excess of rotation rate over the strain rate magnitude in all directions, the λ_2 criterion looks for this excess only on a specific plane (Jeong & Hussain 1995).

From multi-variable calculus, the point of local pressure minimum in a plane requires two eigenvalues of the local pressure Hessian to be positive and the local pressure gradient component on the plane to be zero. The region in which the two eigenvalues of the pressure Hessian are positive (i.e. $\lambda_2 < 0$) is thus less restrictive and may not include the point of planar pressure minimum in its interior (if there does not exist a point of vanishing pressure gradient on the plane). Furthermore, the relationship between the actual pressure distribution and the modified pressure distribution that neglects the unsteady and viscous terms, is not clear. Also, as noted by Cucitore, Quadrio & Baron (1999), the pressure Hessian concept as defined above is not applicable for the case of compressible flows because of non-vanishing density gradient and divergence of velocity.

2.1.3. Δ *criterion*

Using critical point theory Chong *et al.* (1990) define a vortex core to be the region where ∇v has complex eigenvalues. In a non-rotating reference frame translating with a fluid particle, the instantaneous streamline pattern (obtained from Taylor series expansion of the local velocity to a linear order) is governed by the eigenvalues of ∇v. These streamlines are closed or spiralling if two of the eigenvalues form a complex conjugate pair (for both compressible and incompressible flows). In an unsteady flow the usage of instantaneous streamlines implies assuming the velocity field to be frozen at that instant in time.

The characteristic equation for ∇v is given by

$$\lambda^3 + P\lambda^2 + Q\lambda + R = 0, \tag{2.4}$$

where P, Q, and R are the three invariants of ∇v, defined as $P = -\nabla \cdot v$ (first invariant), Q (second invariant defined in §2.1.1), and $R = -\mathrm{Det}(\nabla v)$ (third invariant). The discriminant for equation (2.4) is (for incompressible case, i.e. when $P = 0$)

$$\Delta = \left(\tfrac{1}{2}R\right)^2 + \left(\tfrac{1}{3}Q\right)^3. \tag{2.5}$$

The condition $\Delta > 0$ implies that ∇v has complex eigenvalues. From equation (2.5) it can be seen that the $Q > 0$ criterion is more restrictive than the $\Delta > 0$ criterion (also see figure 2*c*).

2.1.4. *Swirling strength* (λ_{ci}) *criterion*

The 'swirling strength' criterion of Zhou *et al.* (1999) is based on the Δ criterion and uses the imaginary part of the complex conjugate eigenvalue of ∇v to identify vortices. When ∇v has complex conjugate eigenvalues, in the locally curvilinear coordinate system (y_1, y_2, y_3) spanned by the vectors (v_r, v_{cr}, v_{ci}) and locally translating with the

fluid particle, the instantaneous streamlines are given by

$$y_1(t) = y_1(0)e^{\lambda_r t}, \qquad (2.6a)$$

$$y_2(t) = e^{\lambda_{cr} t}[y_2(0)\cos(\lambda_{ci}t) + y_3(0)\sin(\lambda_{ci}t)], \qquad (2.6b)$$

$$y_3(t) = e^{\lambda_{cr} t}[y_3(0)\cos(\lambda_{ci}t) - y_2(0)\sin(\lambda_{ci}t)]. \qquad (2.6c)$$

Here $(\lambda_r, \boldsymbol{v}_r)$ is the real eigenpair and $(\lambda_{cr} \pm i\lambda_{ci}, \boldsymbol{v}_{cr} \pm i\boldsymbol{v}_{ci})$ the complex conjugate eigenpair of $\nabla \boldsymbol{v}$. In a time-frozen field, streamlines are the same as pathlines, and t denotes the time-like parameter that evolves the pathline or streamline. It can be seen that the flow is locally swirling in the plane spanned by $(\boldsymbol{v}_{cr}, \boldsymbol{v}_{ci})$ and is stretched or compressed along $\boldsymbol{v}_r$. The 'swirling strength', given by λ_{ci}, is a measure of the local swirling rate inside the vortex (the time period for completing one revolution of the streamline is given by $2\pi/\lambda_{ci}$). The strength of stretching or compression is determined by λ_r. One distinctive feature of the swirling strength criterion is that it not only identifies the vortex core region, but also identifies the strength and the local plane of swirling. A similar criterion based on complex eigenvalues has been employed by Berdahl & Thompson (1993) in the context of aerodynamic flows. It may be noted that although $\Delta = 0$ and $\lambda_{ci} = 0$ are equivalent, in the case of non-zero thresholds the interpretation can be significantly different (this issue is addressed later in this paper).

2.2. *A non-local approach*

All the criteria discussed in § 2.1 are based on the local analysis of the velocity gradient tensor. The notion of vortex core being a coherent structure in a turbulent flow introduces the concept of a small but bounded flow region with spatially varying vorticity, where the fluid motion remains spatially and temporally coherent. These aspects introduce a non-local variation which goes beyond the point-wise characterization provided by the local analysis of $\nabla \boldsymbol{v}$.

An empirical Galilean invariant non-local criterion proposed by Cucitore *et al.* (1999) uses the intuitive notion that the change in the relative distance between particles inside a vortex structure is small. To quantify this they introduce a ratio

$$D(\boldsymbol{x}, t) = \frac{\left| \int_0^t \boldsymbol{u}_a(\tau)\, \mathrm{d}\tau - \int_0^t \boldsymbol{u}_b(\tau)\, \mathrm{d}\tau \right|}{\int_0^t |\boldsymbol{u}_a(\tau) - \boldsymbol{u}_b(\tau)|\, \mathrm{d}\tau}, \qquad (2.7)$$

where $\boldsymbol{u}_a$ and $\boldsymbol{u}_b$ are the velocities of two fluid particles (a, b) in the flow and $\boldsymbol{x}$ is the position vector of their mid-point location. The numerator of equation (2.7) is the relative distance between the particle pair at time t, and the denominator measures the cumulative magnitude of distance between the particle pair over the same time. This ratio D is a function of the initial position of the particle pair (a, b) and time t. It is bound between 0 and 1, and is a Galilean invariant quantity. For pairs of particles inside a vortical structure, the numerator is not expected to increase much, but the denominator grows steadily with time. Hence, the vortex is identified to be the flow region satisfying D less than some threshold D_{th}. It can be inferred from equation (2.7) that the ratio D remains small even in case of some non-vortical uniform flows. Therefore, Cucitore *et al.* (1999) propose using this criterion in conjunction with the $\Delta > 0$ criterion. The idea is to identify the subset of the locally swirling $\Delta > 0$ region for which the ratio D remains less than a threshold value.

3. New criterion: enhanced swirling strength

3.1. *Criteria for a vortex core*

For a three-dimensional flow, we propose the following requirements for the identification of a vortex core:

 (i) the identification criterion should be Galilean invariant;

 (ii) the local flow in the frame of reference translating with the vortex should be swirling;

 (iii) the separation between the swirling material points inside the vortex core should remain small i.e. the orbits of the material points are compact.

The first requirement is the same as that put forward by Jeong & Hussain (1995). The second requirement is a generalization of the idea of a solid body rotation: the local flow about every point is swirling. For example, in a Rankine vortex, the vortex core is unambiguously defined to be the inner core of solid body rotation, where the local streamlines (in a frame of reference translating with the point) circle around the point. This requirement is related to the net vorticity requirement of Jeong & Hussain (1995). In the region with no vorticity all the criteria indicate the absence of a vortex core. The third requirement demands that the fluid particles in the vortex structure have bounded separation (i.e. they stay close to each other) in order to have a significant effect on the flow, thereby making it worth considering both from dynamic and statistical viewpoints. This requirement is an inherently non-local property and can be seen to be related to the intuitive idea of § 2.2.

The Δ or swirling strength criteria by themselves satisfy only the first two requirements. In combination with a threshold value for D, as employed by Cucitore *et al.* (1999), all three requirements can be satisfied. This approach, however, is computationally more involved as it is non-local in nature and requires the evaluation of particle trajectories. Now we introduce a local approximation of this non-local property.

3.2. *New criterion*

We propose an enhancement to the swirling strength criterion in an attempt to identify the vortex cores that meet all the three requirements stated above. The idea here is to approximate the measure of the non-local orbital compactness based on local analysis of time-frozen flow fields. Consider the projected motion of a fluid particle in the plane of the vortex (i.e. the plane spanned by $(\boldsymbol{v}_{cr}, \boldsymbol{v}_{ci})$). From equations (2.6b) and (2.6c), it can be seen that the time period for one revolution in the vortex plane is $2\pi/\lambda_{ci}$. In this plane, two points initially separated by r_0, after n revolutions around each other will be separated by r_f, where the two distances can be expressed in terms of the eigenvalues of $\nabla \boldsymbol{v}$ as (also see Chong *et al.* 1990)

$$\frac{r_f}{r_0} = \exp\left(2\pi n \frac{\lambda_{cr}}{\lambda_{ci}}\right). \tag{3.1}$$

From equation (3.1) we see that there is an exponential dependence on the ratio $\lambda_{cr}/\lambda_{ci}$. We call this ratio, $\lambda_{cr}/\lambda_{ci}$, the *inverse spiralling compactness*, as it measures the spatial extent of the local spiralling motion. A value of $\lambda_{cr}/\lambda_{ci} = 0$ results in a perfectly circular path, while a positive (or negative) value of the ratio corresponds to a path that spirals outward (or inward) in the plane of the vortex. We propose to use this ratio as a measure of the local orbital compactness in a vortex, i.e. to identify the material points that follow orbits which remain compact during the revolutions.

Figure 1 shows the instantaneous streamlines for two different cases with the same value of λ_{ci}, but with different values of the ratio $\lambda_{cr}/\lambda_{ci}$. In both cases the rotation
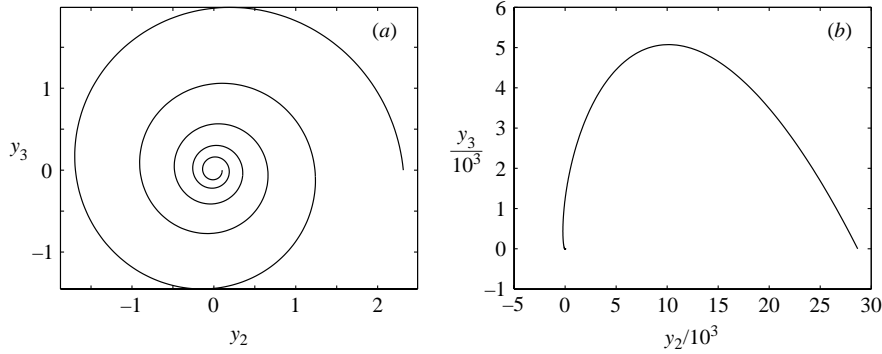
FIGURE 1. Instantaneous streamlines of one revolution for different values of λ_{cr} with a fixed λ_{ci}: (a) $\lambda_{cr} = 0.1$, $\lambda_{ci} = 1$; (b) $\lambda_{cr} = 2$, $\lambda_{ci} = 1$ (note the scale of the axes; although not evident, one complete spiral is shown in the figure). The starting point is taken to be $(y_2(0), y_3(0)) = (0.1, 0)$ and the basis eigenvectors are assumed to be orthogonal.

rate (or angular velocity) remains the same, but for a small value of the ratio, $\lambda_{cr}/\lambda_{ci} = 0.1$, in figure 1(a) we see the behaviour to be consistent with the intuitive notion of a vortex with a spiralling path. On the other hand, for a larger value of the ratio, $\lambda_{cr}/\lambda_{ci} = 2$, figure 1(b) shows the rapid radial spreading out of the instantaneous streamline, which does not appear to qualify as a vortex. It is thus evident that regions of large values of $\lambda_{cr}/\lambda_{ci}$ have low orbital compactness and hence do not qualify as part of a vortex, even though local values of Δ or λ_{ci} might suggest otherwise. Furthermore, in such regions of strong outward spiralling motion, local criteria based on $\nabla \boldsymbol{v}$ become inappropriate, since fluid begins to explore other parts of the flow far from the reference point even as it is completing one full revolution. In particular, in a spatially varying flow with a vortex filament, the fluid particles can be displaced by so much that they experience a significantly different flow environment outside the vortex filament.

For large negative values of the ratio $\lambda_{cr}/\lambda_{ci}$, the instantaneous streamline rapidly spirals inward in the vortex plane. Note that in an incompressible flow, the real eigenvalue and the real part of the complex pair are related as $\lambda_r = -2\lambda_{cr}$. Thus the rapid convergence of particles in the plane of the vortex translates to their rapid separation along the vortex axis. If compactness of material orbit is desired only on the vortex plane, then any negative value of $\lambda_{cr}/\lambda_{ci}$ satisfies the compactness requirement. On the other hand, if compactness of orbit is also desired along the vortex axis, then large negative $\lambda_{cr}/\lambda_{ci}$ violates this requirement. This leads us to two possible ways of defining a vortex core and they are discussed below.

Considering the projected motion on the vortex plane to be the deciding factor, we state the requirements for a point to be considered inside a vortex core as

(i) $\lambda_{ci} \geqslant \epsilon$ and

(ii) $\lambda_{cr}/\lambda_{ci} \leqslant \delta$,

where ϵ and δ are positive thresholds. In other words, the vortex core is the intersection set of the sets defined by $\lambda_{ci} \geqslant \epsilon$ and $\lambda_{cr}/\lambda_{ci} \leqslant \delta$ (refer to figure 8). Here we take λ_{ci} to be always defined non-negative. The first condition can be interpreted as a statement of rate of rotation in the vortex core. Small values of λ_{ci} correspond to long times to complete a revolution and imply a weak vortex region. Similarly large λ_{ci} values imply a strong vortex region. As argued above, the second criterion on the ratio $\lambda_{cr}/\lambda_{ci}$ can be interpreted as the corresponding statement on the orbital compactness
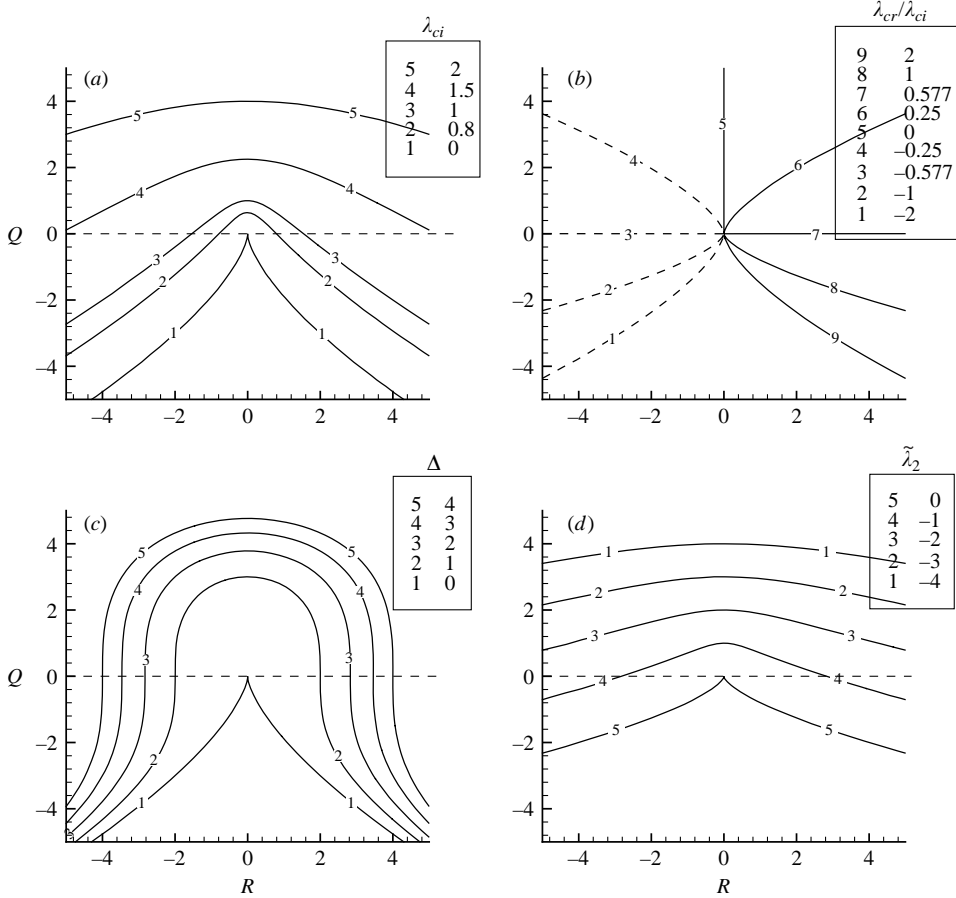
FIGURE 2. Contour lines (i.e. lines of constant function values) in the (Q, R)-plane:
(a) λ_{ci}; (b) $\lambda_{cr}/\lambda_{ci}$ (dashed lines represent negative contours); (c) Δ; (d) $\tilde{\lambda}_2$.

of the vortex core. Large values of $\lambda_{cr}/\lambda_{ci}$ imply that initially close particles do not remain neighbours (in the plane of the vortex) after the time that has elapsed for a complete revolution. The values of ϵ and δ depend on the level of swirling rate and vortex-plane orbital compactness that we require to qualify as a vortex core.

When orbital compactness is desired both on the vortex plane and along the vortex axis (i.e. compactness in the three-dimensional space), for an incompressible flow the vortex core requirements are

(i) $\lambda_{ci} \geqslant \epsilon$ and

(ii) $-\kappa \leqslant \lambda_{cr}/\lambda_{ci} \leqslant \delta$,

where κ is a positive threshold and its value depends on the desired orbital compactness along the vortex axis. The above requirement can be easily generalized for compressible flows.

4. Relation between the different criteria

Both the swirling strength, λ_{ci}, and the inverse spiralling compactness, $\lambda_{cr}/\lambda_{ci}$, are uniquely determined in terms of the three scalar invariants of ∇v (see equation (2.4)). In the special case of an incompressible flow they depend only on the second and

third invariants, i.e. on Q and R (refer to figures 2(a) and 2(b) for the contour lines in the (Q, R)-plane). It is known that for a two-dimensional incompressible flow the Q, λ_2, and λ_{ci} criteria result in the same vortex core region (Jeong & Hussain 1995). In this section, for a three-dimensional incompressible flow, we seek to establish the relation between the different criteria by expressing them in terms of λ_{ci} and $\lambda_{cr}/\lambda_{ci}$.

4.1. *Relation to the Q criterion*

In incompressible flows, the region of $Q > 0$ is a subset of the region defined by $\lambda_{ci} > 0$, and the second invariant can be explicitly written as

$$Q = \lambda_{ci}^2 \left(1 - 3 \left(\frac{\lambda_{cr}}{\lambda_{ci}} \right)^2 \right). \tag{4.1}$$

This indicates that $Q > 0$ can be interpreted as the region with local swirling ($\lambda_{ci} > 0$) where the local inward and outward spiralling is limited by $|\lambda_{cr}/\lambda_{ci}| < 1/\sqrt{3}$. Thus the $Q > 0$ criterion will avoid regions of strong outward spiralling given by $\lambda_{cr}/\lambda_{ci} > 1/\sqrt{3}$. This will, however, also avoid regions of strong inward spiralling marked by $\lambda_{cr}/\lambda_{ci} < -1/\sqrt{3}$, for e.g. vortices that are undergoing rapid intensification by axial strain.

4.2. *Relation to the Δ criterion*

In incompressible flows, the discriminant Δ can be written as

$$\Delta = \frac{\lambda_{ci}^6}{27} \left[1 + 9 \left(\frac{\lambda_{cr}}{\lambda_{ci}} \right)^2 \right]^2. \tag{4.2}$$

For small values of $\lambda_{cr}/\lambda_{ci}$, we have the following behaviour:

$$\Delta/\lambda_{ci}^6 \to (1/27) + (2/3)(\lambda_{cr}/\lambda_{ci})^2.$$

Thus, Δ/λ_{ci}^6 takes the lowest value of $(1/27)$ when the local flow is purely circular, i.e. when $\lambda_{cr}/\lambda_{ci} = 0$, and quadratically increases with the ratio $\lambda_{cr}/\lambda_{ci}$ as the local flow spirals in or out. The limit $\Delta = 0$ is identical to the $\lambda_{ci} = 0$ condition. Nevertheless, differences emerge with the use of a small positive threshold. From equation (4.2) it is clear that a $\Delta > \Delta_{th}$ criterion can be satisfied even when λ_{ci} is very small provided the ratio $|\lambda_{cr}/\lambda_{ci}|$ is sufficiently large. In other words, very weak swirling motion along with intense radial divergence (or convergence) in the plane of swirl, could qualify as a strong vortex. Furthermore, similarly to the Q criterion, the Δ criterion also does not distinguish between the inward and outward spiralling motion. Figure 2(c) shows the contour lines of Δ in the (Q, R)-plane (equation (2.5)).

4.3. *Relation to the λ_2 criterion*

The λ_2 criterion cannot be expressed solely in terms of the eigenvalues of $\nabla \boldsymbol{v}$, or its scalar invariants, as the value of λ_2 for a given $\nabla \boldsymbol{v}$ depends also on the eigenvectors of $\nabla \boldsymbol{v}$ (see the Appendix). Similarly to the Q and Δ criteria, the λ_2 criterion does not distinguish between the regions of inward and outward spiralling motion.

4.3.1. *Generic characterization of the $\lambda_2 < 0$ region*

In order to fully explore the relation between λ_2 and the eigenvalues (or the scalar invariants) of $\nabla \boldsymbol{v}$, we explore all the possible configurations of $\nabla \boldsymbol{v}$ for incompressible flows. Consider the reference coordinate axes to be aligned along the principal directions of the strain-rate tensor (symmetric part of $\nabla \boldsymbol{v}$). The eigenvalues of the
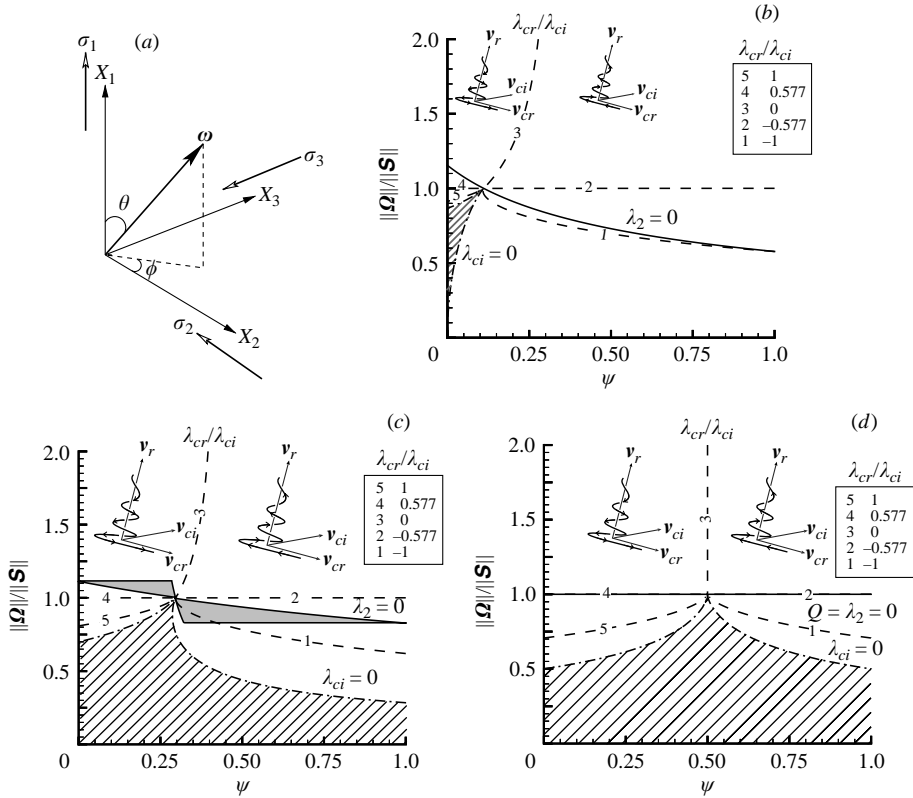
FIGURE 3. (*a*) Configuration of the generic characterization problem; vortex region in the $(\|\boldsymbol{\Omega}\|/\|\boldsymbol{S}\|, \psi)$-space for different values of ξ: (*b*) $\xi = 1$; (*c*) $\xi = 0.5$; (*d*) $\xi = 0$. The contour lines indicate: $\lambda_{ci} = 0$ (– · – · –), $\lambda_2 = 0$ (——), and $\lambda_{ci}/\lambda_{cr}$ (– – –) (see legend box). The region of real eigenvalues of ∇v is shown hatched.

strain-rate tensor can be written as $\sigma_1 \geqslant \sigma_2 \geqslant \sigma_3$, where $\sigma_1 + \sigma_2 + \sigma_3 = 0$ (incompressibility). When $\sigma_1 \geqslant -\sigma_3$, defining the coordinate system as depicted in figure 3(*a*), the strain-rate tensor can be written as

$$\boldsymbol{S} = \sigma_1 \begin{bmatrix} 1 & 0 & 0 \\ 0 & -\xi/2 & 0 \\ 0 & 0 & \xi/2 - 1 \end{bmatrix}, \tag{4.3}$$

where ξ determines the nature of the strain field. In the case of $\sigma_1 \geqslant -\sigma_3$, there is converging flow in the (X_2, X_3)-plane and $0 \leqslant \xi \leqslant 1$. Here $\xi = 0$ corresponds to planar strain and $\xi = 1$ corresponds to axisymmetric converging strain. The skew-symmetric part of the velocity gradient tensor is governed by the vorticity vector $\boldsymbol{\omega}$ superposed on the strain flow. Within a scaling factor, the velocity gradient tensor can be written as

$$\nabla v = \begin{bmatrix} 1 & -a \sin\theta \sin\phi & a \sin\theta \cos\phi \\ a \sin\theta \sin\phi & -\xi/2 & -a \cos\theta \\ -a \sin\theta \cos\phi & a \cos\theta & \xi/2 - 1 \end{bmatrix}, \tag{4.4}$$

where $a = |\boldsymbol{\omega}|/2\sigma_1$ (always non-negative by definition); θ and ϕ define the orientation of the vorticity vector (see figure 3*a*). The relative strength of rotation rate compared to strain rate, $\|\boldsymbol{\Omega}\|/\|\boldsymbol{S}\|$, is given by $\sqrt{2}a/\sqrt{\xi^2/2 - \xi + 2}$. When $\sigma_1 < -\sigma_3$, we define

the coordinate directions (X_1, X_2, X_3) along $(\sigma_3, \sigma_2, \sigma_1)$. In this case, there is diverging flow in the (X_2, X_3)-plane and $-1 \leqslant \xi < 0$, where $\xi = -1$ corresponds to axisymmetric diverging strain. By keeping the definition of the skew-symmetric part unchanged it can be shown that the eigenvalues of ∇v for $\xi < 0$ are equal to the negative of the eigenvalues for positive ξ of the same magnitude. Hence, analysing the ∇v configurations for $\xi \geqslant 0$ is sufficient.

By varying $0 \leqslant \|\boldsymbol{\Omega}\|/\|\boldsymbol{S}\| < \infty$, $0 \leqslant \xi \leqslant 1$, $0 \leqslant \theta \leqslant \pi$, and $0 \leqslant \phi \leqslant 2\pi$, all the possible configurations of ∇v are covered and over this range one can compute the region of $\lambda_2 < 0$ and compare with regions of $\lambda_{ci} > 0$, $Q > 0$, and the range of $\lambda_{cr}/\lambda_{ci}$. It may be noted that these relationships are independent of the scaling factor for ∇v. From the definition of the invariants of ∇v it can be seen that Q depends only on ξ and $\|\boldsymbol{\Omega}\|/\|\boldsymbol{S}\|$, and is independent of the orientation angles. Also, by definition, the third invariant R depends on ξ, $\|\boldsymbol{\Omega}\|/\|\boldsymbol{S}\|$, and ψ, where ψ is formed by combining the angles θ and ϕ as

$$\psi = \frac{3 \cos 2\theta - 2(\xi - 1) \cos 2\phi \sin^2 \theta - (2\xi - 5)}{2(4 - \xi)}. \tag{4.5}$$

Hence, the eigenvalues of ∇v are now dependent only on $\|\boldsymbol{\Omega}\|/\|\boldsymbol{S}\|$, ξ, and ψ (where $0 \leqslant \psi \leqslant 1$). Figure 3($b$–$d$) shows the contour lines of $\lambda_{cr}/\lambda_{ci}$ plotted as a function of $\|\boldsymbol{\Omega}\|/\|\boldsymbol{S}\|$ and ψ for three types of strain flows (determined by ξ). Note that $\Delta = 0$ (or $\lambda_{ci} = 0$) corresponds to $\lambda_{cr}/\lambda_{ci} \to \infty$; $Q = 0$ corresponds to $\lambda_{cr}/\lambda_{ci} = \pm 1/\sqrt{3}$, which is identical to the condition $\|\boldsymbol{\Omega}\|/\|\boldsymbol{S}\| = 1$. We are particularly interested in exploring the range of $\lambda_{cr}/\lambda_{ci}$ corresponding to $\lambda_2 < 0$, which in turn indicates the threshold imposed by $\lambda_2 < 0$ on the inward or outward spiralling motion. Now we discuss the different strain flows and thereafter summarize our findings.

(i) $\xi = 1$: axisymmetric radial convergence

We first consider the case of axisymmetric strain rate, with axisymmetric radial convergence along the (X_2, X_3)-plane and axial divergence along the X_1-axis. In this strain configuration $\psi = \cos^2 \theta$ and hence the results are independent of the angle ϕ. The $\lambda_{ci} = 0$ contour line has two branches that exist over the range $0 < \psi \lesssim 0.12$. Between the two branches all three eigenvalues of ∇v are real, and outside the two branches a complex eigenpair exists. According to the $\lambda_{ci} > 0$ criterion, in the range $0 < \psi \lesssim 0.12$ a vortex exists even for infinitesimally small values of $\|\boldsymbol{\Omega}\|/\|\boldsymbol{S}\|$, but with increasing relative vorticity magnitude the vortex disappears and reappears again above a certain relative vorticity magnitude. This behaviour is clearly counterintuitive and we call this the *disappearing vortex problem*. Investigating the region below the lower branch reveals that the nature of swirling is quite unusual here. The plane of swirling, as identified by the complex eigenvectors, is such that its normal is not nearly aligned with the local vorticity vector, but in fact nearly orthogonal to it. In contrast, in the region above the upper branch, where the relative magnitude of vorticity is substantial, the normal to the plane of swirling and the real eigenvectors are aligned close to the vorticity vector, as can be expected of a strong vortical region. Furthermore, the value of the inverse spiralling compactness, $\lambda_{cr}/\lambda_{ci}$, takes large negative values in the region below the lower branch. This region can be eliminated from the vortex core if there is a restriction imposed on the orbital compactness along the vortex axis, i.e. using $\lambda_{cr}/\lambda_{ci} \geqslant -\kappa$.

When the vorticity vector is perfectly aligned along the axis of the axisymmetric strain rate (X_1-axis), $\psi = 1$, and in this limit $\lambda_2 = 0$ corresponds to $\lambda_{cr}/\lambda_{ci} = -1$ and a relative rotation rate magnitude of $\|\boldsymbol{\Omega}\|/\|\boldsymbol{S}\| \approx 0.58$. As the alignment is changed by

increasing θ (or decreasing ψ), the inverse spiralling compactness and relative rotation rate (that correspond to the $\lambda_2 = 0$ contour line) increase: for $\psi \approx 0.12$ we approach the limit $\lambda_{cr}/\lambda_{ci} \to -1/\sqrt{3}$ and $\|\boldsymbol{\Omega}\|/\|\boldsymbol{S}\| \to 1$. Over the range $0.12 \lesssim \psi \leqslant 1$ the $Q > 0$ criterion yields only a subset of the vortex extracted by the $\lambda_2 < 0$ criterion, since for the same value of ψ the $Q > 0$ condition is satisfied only at a larger $\|\boldsymbol{\Omega}\|/\|\boldsymbol{S}\|$. In other words, the $\lambda_2 < 0$ criterion is less restrictive than the $Q > 0$ criterion in this range of ψ values. The case of $\psi \approx 0.12$ and $\|\boldsymbol{\Omega}\|/\|\boldsymbol{S}\| = 1$ corresponds to a generalized shear layer with all three eigenvalues of $\nabla \boldsymbol{v}$ becoming identically zero. As a result, the ratio $\lambda_{cr}/\lambda_{ci}$ is indeterminate at this point and results in a cusp. For ψ from ~ 0.12 to 0, the $\lambda_2 = 0$ contour line is equivalent to a positive value of $\lambda_{cr}/\lambda_{ci}$ over the range from $1/\sqrt{3}$ to ~ 0.4 and correspondingly demands a stronger relative rotation rate, $\|\boldsymbol{\Omega}\|/\|\boldsymbol{S}\|$, from 1.0 to ~ 1.15. Over the range $0 \leqslant \psi \lesssim 0.12$, the $\lambda_2 < 0$ criterion is more restrictive than the $Q > 0$ criterion.

(ii) $\xi = 0.5$

In this case the strain rate is neither axisymmetric nor planar. The $\lambda_{ci} = 0$ contour line still shows signs of the disappearing vortex problem over a narrow range of $0.28 \lesssim \psi \lesssim 0.31$. The behaviour of the two swirling regions between the lower branches and above the upper branch is quite different. In particular the region of $\lambda_{ci} > 0$ that exists between the lower branches is associated with large negative values of $\lambda_{cr}/\lambda_{ci}$ and thus can be eliminated if orbital compactness requirement is imposed along the vortex axis.

$\psi = 1$ corresponds to the vorticity vector orientation $\theta = 0$ and is independent of ϕ. For this orientation the $\lambda_2 = 0$ contour line is equivalent to $\lambda_{cr}/\lambda_{ci} \approx -0.78$ and $\|\boldsymbol{\Omega}\|/\|\boldsymbol{S}\| \approx 0.81$. As can be seen from equation (4.5), varying combinations of θ and ϕ can lead to the same value for ψ, and therefore for a fixed ψ the $\lambda_2 = 0$ contour line covers a range of $\|\boldsymbol{\Omega}\|/\|\boldsymbol{S}\|$ and correspondingly a range of $\lambda_{cr}/\lambda_{ci}$. This range is indicated in figure 3(b) as the shaded region. For $1 \geqslant \psi \gtrsim 0.31$, the $\lambda_2 < 0$ region extends over the range $-1.3 \lesssim \lambda_{cr}/\lambda_{ci} < -1/\sqrt{3}$ and is less restrictive than $Q > 0$. The case of $\psi \approx 0.31$ and $\|\boldsymbol{\Omega}\|/\|\boldsymbol{S}\| = 1$ corresponds to a generalized shear layer. For $0.31 \gtrsim \psi \geqslant 0$, the $\lambda_2 < 0$ region covers the range $1/\sqrt{3} > \lambda_{cr}/\lambda_{ci} \gtrsim 0.3$ and is more restrictive than $Q > 0$.

(iii) $\xi = 0$: Planar strain

Here the plane of strain is the (X_1, X_3)-plane. Note that in this limit the problem of the disappearing vortex is absent. The particular case of $\theta = \phi = \pi/2$ corresponds to the classic two-dimensional shear layer. The point of cusp given by $\psi = 0.5$ and $\|\boldsymbol{\Omega}\|/\|\boldsymbol{S}\| = 1$ is again the generalized shear layer where the eigenvalues of $\nabla \boldsymbol{v}$ are identically zero. The condition $\lambda_2 = 0$ corresponds to $|\lambda_{cr}/\lambda_{ci}| = 1/\sqrt{3}$ and $\|\boldsymbol{\Omega}\|/\|\boldsymbol{S}\| = 1$. Thus, for planar strain, irrespective of vorticity orientation, the $\lambda_2 < 0$ criterion is identical to the $Q > 0$ criterion.

(iv) Summary of observations

Based on the above discussion, it is clear that the $\lambda_2 < 0$ region corresponds to a range of positive and negative $\lambda_{cr}/\lambda_{ci}$, indicating a threshold on both outward and inward spiral regions. Although there is no unique relation between λ_2 and $\lambda_{cr}/\lambda_{ci}$, an investigation of the configurational space shows that the $\lambda_2 < 0$ region is approximately bracketed by the range $-O(1) \lesssim \lambda_{cr}/\lambda_{ci} \lesssim O(1)$. Note that there are a few cases where $\lambda_{cr}/\lambda_{ci}$ can take very high values or be undefined (see §4.3.2 for the range where $\lambda_{cr}/\lambda_{ci}$ is undefined). Also note that all the criteria agree on the presence of a vortex in the intense vortical regions (i.e. for high values of $\|\boldsymbol{\Omega}\|/\|\boldsymbol{S}\|$). The differences emerge in the regions where $\|\boldsymbol{\Omega}\|/\|\boldsymbol{S}\|$ is small. Hence, the different schemes disagree mainly on the boundary of the vortex core.
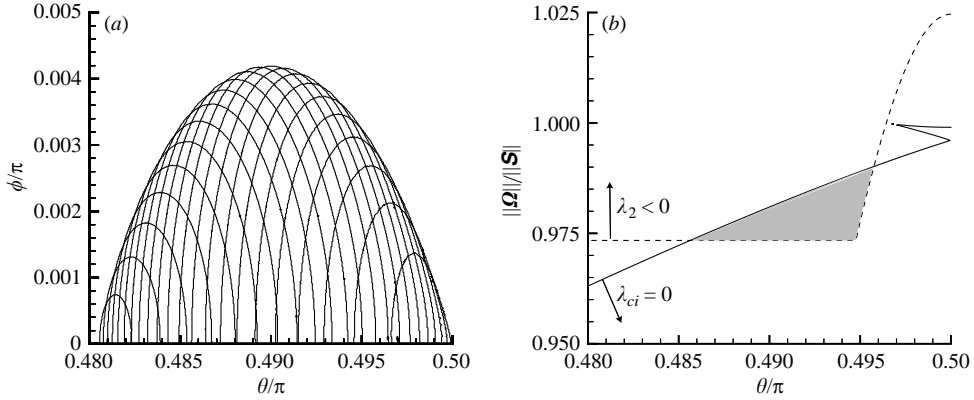
FIGURE 4. (*a*) Region in (θ, ϕ)-plane where $\lambda_2 < 0$ and $\lambda_{ci} = 0$. The curves represent varying ξ values from 0.01 (rightmost) to 0.22 (leftmost), with an increment of 0.01. (*b*) For a horizontal slice (at $\phi = 0$) through the curve for $\xi = 0.1$ in frame (*a*), the shaded area in this frame represents the region of $\lambda_{ci} = 0$ and $\lambda_2 < 0$ in $(\theta, \|\boldsymbol{\Omega}\|/\|\boldsymbol{S}\|)$-space.

4.3.2. *The largest vortex region*

Here we compare the size of the vortex region extracted by the $\lambda_{ci} > 0$ (or $\Delta > 0$) criterion with that by the $Q > 0$ and $\lambda_2 < 0$ criteria. In figure 3(*b–d*), both the $Q > 0$ and $\lambda_2 < 0$ conditions never extend into the region of all three real eigenvalues of $\nabla \boldsymbol{v}$. Hence, it is tempting to conjecture that the flow region defined by $\lambda_{ci} > 0$ captures the largest vortex region. It was noted earlier that the vortex region identified by $\lambda_{ci} > 0$ is guaranteed to be larger than or equal to that extracted by $Q > 0$. Alternatively, the same conclusion can be deduced from the equivalence of $Q = 0$ and $|\lambda_{ci}/\lambda_{cr}| = 1/\sqrt{3}$. In the case of the λ_2 criterion, however, there exists a very narrow range of configuration of $\nabla \boldsymbol{v}$ for which λ_2 is negative, while all the eigenvalues of $\nabla \boldsymbol{v}$ are real. The limited extent of this possibility in the configuration space is shown in figure 4(*a*). Each curve corresponds to a constant value of ξ and the region inside the curve defines the range of θ, ϕ combination (for some range of $\|\boldsymbol{\Omega}\|/\|\boldsymbol{S}\|$) for which a vortex is predicted according to the $\lambda_2 < 0$ criterion, but not by the $\lambda_{ci} > 0$ criterion. In this region, the $\lambda_2 < 0$ criterion predicts a vortex in a region where there is no local swirling. This possibility is further illustrated in figure 4(*b*), where the contour lines of $\lambda_2 = 0$ and $\lambda_{ci} = 0$ are plotted for a range of θ and $\|\boldsymbol{\Omega}\|/\|\boldsymbol{S}\|$, at a fixed value of $\xi = 0.1$ and $\phi = 0$. A narrow region (shaded in the figure) can be identified over which the $\lambda_2 < 0$ criterion predicts a vortex where local swirling does not exist. Thus for a small range of ξ close to planar strain ($0 < \xi \lesssim 0.22$), over a very small range of vorticity orientation where the vorticity vector is almost normal to the plane of strain ($\theta \approx \pi/2$, $\phi \approx 0$), and for a narrow range of vorticity magnitude approximately equal to that of strain rate ($\|\boldsymbol{\Omega}\|/\|\boldsymbol{S}\| \approx 1$), while $\lambda_2 < 0$ criterion signals a vortex, the $\lambda_{ci} > 0$ criterion does not. By symmetry, in the $\xi < 0$ regime as well, over a narrow range in configuration space, λ_2 takes negatives values, even though there is no swirling in the flow according to λ_{ci}. Note that a planar strain with $\theta = \pi/2$, $\phi = 0$, and $\|\boldsymbol{\Omega}\|/\|\boldsymbol{S}\| = 1$ corresponds to a two-dimensional shear flow. From the limited extent of this region of $\lambda_2 < 0$ with $\lambda_{ci} = 0$, it appears reasonable to conclude that for all practical purposes the $\lambda_{ci} > 0$ condition will extract the largest vortex core among all the criteria considered. In our experience with actual turbulent flow data, we see that the region of $\lambda_{ci} > 0$ does indeed extract the largest vortex core region, implying that in turbulent flows the configuration depicted in figure 4 seldom occurs.

4.3.3. *Special case formulation: orthonormal eigen-basis vectors*

It was noted earlier that λ_2 cannot be determined from the invariants of ∇v because of its additional dependence on the orientation of the eigenvectors of ∇v. Nevertheless, in the special case when the eigen-basis vectors (v_r, v_{cr}, v_{ci}) are orthonormal, λ_2 can be expressed in terms of the eigenvalues of ∇v as

$$\lambda_2 = \tilde{\lambda}_2 = \lambda_{ci}^2 \left(\left(\frac{\lambda_{cr}}{\lambda_{ci}} \right)^2 - 1 \right). \tag{4.6}$$

Hence, for this case, the $\lambda_2 < 0$ condition is equivalent to $|\lambda_{cr}/\lambda_{ci}| < 1$.

It may be noted that the real-valued ∇v being a normal tensor (i.e. $(\nabla v) \cdot (\nabla v)^T = (\nabla v)^T \cdot (\nabla v)$) is a necessary and a sufficient condition for the eigen-basis vectors to be orthonormal. The condition $\lambda_2 = \tilde{\lambda}_2$, is not accurate when the eigen-basis vectors of ∇v are not orthonormal. Nevertheless, even in such cases we will use $\tilde{\lambda}_2$ as a proxy for λ_2. In figure 3, the $\tilde{\lambda}_2 = 0$ contour line is represented by $|\lambda_{cr}/\lambda_{ci}| = 1$ (i.e. $\lambda_{cr}/\lambda_{ci}$ contour numbers 1 and 5). For the case of axisymmetric radial convergent strain ($\xi = 1$), in the region of outward spiral marked by positive values for the ratio $\lambda_{cr}/\lambda_{ci}$, $\tilde{\lambda}_2 = 0$ appears to provide a good approximation for $\lambda_2 = 0$. In the inward spiral region, $\tilde{\lambda}_2 = 0$ is less restrictive than $\lambda_2 = 0$. A similar behaviour is observed for the case of $\xi = 0.5$. In the planar case ($\xi = 0$), $\tilde{\lambda}_2 = 0$ is less restrictive than $\lambda_2 = 0$ for both the inward and outward spiral regions.

4.4. *Simple examples*

4.4.1. *Isolated Burgers' vortex*

Here we discuss the vortex core of the radially symmetric Burgers' vortex (Burgers 1948). This vortex has been widely used for modelling fine scales of turbulence (Pullin & Saffman 1998). The Burgers' vortex is an exact steady solution of the Navier–Stokes equation, where the radial viscous diffusion of vorticity is dynamically balanced by vortex stretching due to an axisymmetric strain. The velocity components in cylindrical coordinates for a Burgers' vortex can be written as

$$v_r = -\xi r, \tag{4.7a}$$

$$v_\theta = \frac{\Gamma}{2\pi r} \left[1 - \exp\left(\frac{-r^2 \xi}{2\nu} \right) \right], \tag{4.7b}$$

$$v_z = 2\xi z, \tag{4.7c}$$

where Γ is the circulation, ξ the axisymmetric strain rate, and ν the kinematic viscosity. The Reynolds number for the vortex can be defined as $Re = \Gamma/(2\pi\nu)$.

In this simple flow field, the various vortex identification criteria can be analytically expressed as

$$\lambda_{ci} = Re\xi\sqrt{\eta(\tilde{r})} \quad \text{and} \quad \lambda_{cr}/\lambda_{ci} = -\frac{1}{Re\sqrt{\eta(\tilde{r})}}, \tag{4.8a}$$

$$Q = \xi^2 (Re^2 \eta(\tilde{r}) - 3), \tag{4.8b}$$

$$\Delta = \frac{\xi^6 Re^2 \eta(\tilde{r})}{27} [9 + Re^2 \eta(\tilde{r})]^2, \tag{4.8c}$$

$$\lambda_2 = \xi^2 \left[1 - Re^2 \eta(\tilde{r}) - \frac{Re}{\tilde{r}^2} \left((2 + \tilde{r}^2) e^{-\tilde{r}^2/2} - 2 \right) \right], \tag{4.8d}$$

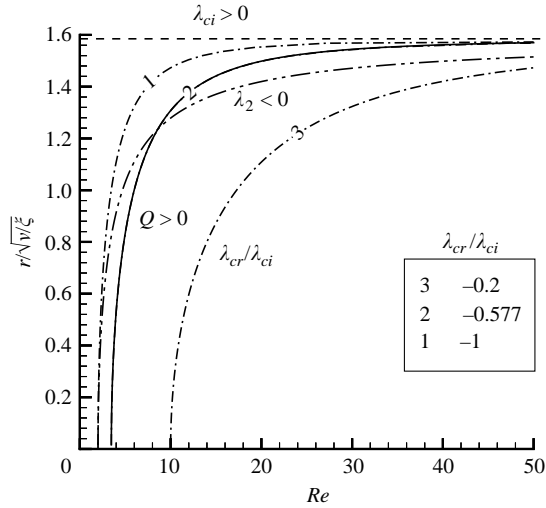$$\tilde{\lambda}_2 = \xi^2 (1 - Re^2 \eta(\tilde{r})), \tag{4.8e}$$

FIGURE 5. Radius of a Burgers' vortex core according to: $\lambda_{ci} > 0$ or $\Delta > 0$ $(- - -)$,
$Q > 0$ (———), $\lambda_2 < 0$ $(\cdots\cdots)$, and $\lambda_{cr}/\lambda_{ci}$ $(- \cdot - \cdot -)$ (see legend box).

where $\tilde{r} = \sqrt{\xi/\nu}$ and the auxiliary function $\eta(\tilde{r})$ is defined as

$$\eta(\tilde{r}) = \frac{1}{\tilde{r}^4}\left((1 + \tilde{r}^2)e^{-\tilde{r}^2/2} - 1\right)\left(1 - e^{-\tilde{r}^2/2}\right).$$

The $\lambda_{ci} > 0$ condition simply translates to $\eta(\tilde{r}) > 0$ and yields a non-dimensional vortex size of $r_0\sqrt{\xi/\nu} \approx 1.585$, which is independent of the Reynolds number. Interestingly, the radial distribution of circumferential velocity peaks precisely at this radial location. Thus, as in the case of Rankine vortex, the circumferential velocity radially increases within the vortex core and outside the vortex core the circumferential velocity decays as a point vortex. In the core region identified by $\lambda_{ci} > 0$, the values of $\lambda_{cr}/\lambda_{ci}$ are negative everywhere, hence the local flow is spiralling inward in the plane of the vortex. If orbital compactness is desired only on the vortex plane, then the vortex core is independent of the values of $\lambda_{cr}/\lambda_{ci}$. Additionally, if compactness is desired along the vortex axis too, then the choice the threshold κ makes the vortex core radius a function of Re. From equation (4.8a), we see that $\lambda_{cr}/\lambda_{ci} \sim -1/Re$, which implies that at large Reynolds numbers the vortex size will not be sensitively dependent on the threshold κ.

Figure 5 shows the non-dimensional vortex radius as a function of Re implied by the different criteria. It can be easily verified that for $Re < 2\sqrt{3}$, Q is negative for all radii r and thus for $Re < 2\sqrt{3}$ there is no vortex core according to $Q > 0$ criterion. As the Reynolds number increases above this value, the radius of the vortex core (identified by $Q > 0$) increases, and the limit $Re \to \infty$ yields $r_{Q>0} \to r_0$. As discussed in §4.1, the $Q = 0$ condition is identical to $|\lambda_{cr}/\lambda_{ci}| = 1/\sqrt{3}$ (see contour number 2).

The $\lambda_2 < 0$ criterion also has a lower Reynolds number limit for the existence of a vortex core: for $Re < 2$, $\lambda_2 > 0$ at all radial locations. As Reynolds number increases above this limit, the radius of the vortex core (identified by $\lambda_2 < 0$) increases, and the limit $Re \to \infty$ yields $r_{\lambda_2<0} \to r_0$. Unlike $Q = 0$, however, $\lambda_2 = 0$ does not correspond to a fixed $\lambda_{cr}/\lambda_{ci}$ ratio. As Re ranges from 2 to ∞, the $\lambda_2 = 0$ curve corresponds to a range of $\lambda_{cr}/\lambda_{ci}$ from -1 to 0.
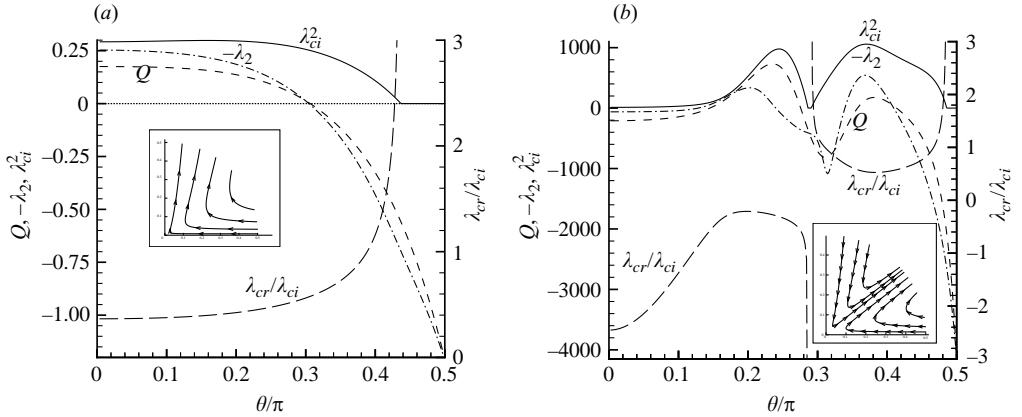
FIGURE 6. (a) Consolidated jet ($M = 3.85$, $\Gamma_0 = 1$): $r^4\lambda_{ci}^2/\nu^2$ (———), r^4Q/ν^2 (– – – –), $-r^4\lambda_2/\nu^2$ (– · – · –), and $\lambda_{cr}/\lambda_{ci}$(– – –). (b) Two-cell pattern ($M = 0.99$, $\Gamma_0 = 30$): $r^4\lambda_{ci}^2/\nu^2$ (———), r^4Q/ν^2 (– – – –), $-r^4\lambda_2/\nu^2$ (– · – · –), and $\lambda_{cr}/\lambda_{ci}$(– – –). The inset in both the figures depicts the motion in the meridional plane.

For the case of $Re \to \infty$, the behaviour of the limits $r_{Q>0} \to r_0$ and $r_{\lambda_2<0} \to r_0$ is to be expected because $\lambda_{cr}/\lambda_{ci} \to 0$ (since $\lambda_{cr}/\lambda_{ci} \sim -1/Re$): for $\lambda_{cr}/\lambda_{ci} = 0$ the flow becomes two-dimensional and all the criteria agree.

4.4.2. *Swirling jet*

Jeong & Hussain (1995) discuss the problem of a swirling jet emerging from a point source of axial momentum and circulation into a half-space. The flow is conically symmetric and a solution of the incompressible Navier–Stokes equation. This problem was used to highlight the differences between the Δ, Q, and λ_2 criteria for identifying vortex cores. Here we explore the relation between the different criteria in terms of the ratio $\lambda_{cr}/\lambda_{ci}$.

We set up the problem following the formulation in Shtern & Hussain (1993). Our numerical approach, however, differs: we use the Newton–Kantorivich method with a Chebyshev grid in the interval $0 \leqslant \cos\theta \leqslant 1$. Here θ is the polar angle (in spherical coordinates) measured from the axis of the jet. Shtern & Hussain (1993) identify two different topologies of the solution based on the meridional motion: (a) a 'consolidated jet', having a strong upward swirling helical jet (see the inset in figure 6a), and (b) a 'two-cell pattern', having a downward near-axis flow with a conical outflow at an angle from it (see the inset in figure 6b). The flow topology depends on two parameters: a measure of the relative strength of axial momentum flux to circulation, M, and swirl Reynolds number, Γ_0 (see Shtern & Hussain 1993, for their definition). From the solution map presented in Shtern & Hussain (1993, figure 19), we choose two points in the parameter plane (M, Γ_0) corresponding to the two distinct flow topologies: consolidated jet (3.85, 1) and two-cell pattern (0.99, 30).

In the case of a consolidated jet (figure 6a), the $Q > 0$ and $\lambda_2 < 0$ criteria identify vortex cores of similar size, whereas the $\lambda_{ci} > 0$ criterion identifies a substantially larger vortex core that extends up to $\theta \approx 0.44\pi$. For the two-cell pattern (figure 6b), according to the $\lambda_{ci} > 0$ criterion almost the entire flow qualifies as vortex core. In contrast, both the $Q > 0$ and $\lambda_2 < 0$ criteria extract two distinct vortex cells within the flow. In this case, the vortex cores identified by the $Q > 0$ and $\lambda_2 < 0$ criteria are not
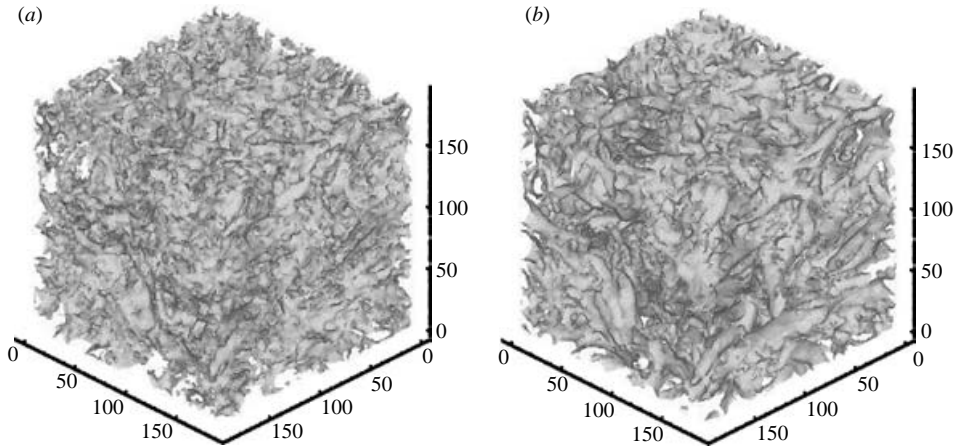
FIGURE 7. Vortex structure using zero threshold for forced isotropic turbulence at $Re_\lambda = 164$. The volume represented is $(1/4)^3$ of the simulation box. (a) $\lambda_{ci} > 0$ or $\Delta > 0$; (b) $\lambda_2 < 0$. The vortex structure for $Q > 0$ looks similar to these figures.

in perfect agreement. These differences in the vortex cores identified by the different criteria are in agreement with the observations of Jeong & Hussain (1995).

The inverse spiralling compactness, $\lambda_{cr}/\lambda_{ci}$, can be used to explain these differences. In figure 6(a), it can be observed that for θ larger than about 0.3π, the ratio $\lambda_{cr}/\lambda_{ci}$ rapidly increases. In this range of θ, even though $\lambda_{ci} > 0$ suggests local swirling, the instantaneous streamlines will strongly spiral out and violate the condition of spatial compactness. With an additional sensible threshold on $\lambda_{cr}/\lambda_{ci}$, the $\lambda_{ci} > 0$ criterion can yield vortex cores comparable to that identified by the $Q > 0$ and $\lambda_2 < 0$ criteria. Thus, in this case, the vortex core identified by the $Q > 0$ and $\lambda_2 < 0$ criteria can be interpreted as swirling regions with an additional constraint on the strength of outward spiralling.

Similarly, in figure 6(b), with a $\lambda_{cr}/\lambda_{ci}$ threshold, what appears to be a single vortex system for the $\lambda_{ci} > 0$ criterion, will become a split vortex system as identified by the other two criteria. A positive threshold for $\lambda_{cr}/\lambda_{ci}$ limits the outward spiralling motion, and hence limits the size of the vortex cell that is closer to the jet plane. Similarly, a negative threshold for $\lambda_{cr}/\lambda_{ci}$ that limits the strength of inward spiralling motion, limits the core size of the vortex close to the jet axis. In essence, the differences between the vortex structures extracted by the different criteria can be interpreted as a consequence of the varying limits these criteria implicitly place on the level of acceptable inward or outward spiralling motion. As a result, with appropriate positive and negative thresholds for $\lambda_{cr}/\lambda_{ci}$, the λ_{ci} criterion can be made to reproduce the results of other criteria.

5. Non-zero threshold

The above discussion of the different criteria has been centred on the zero threshold. While this is a possibility for visualizing vortex cores in simple laminar flows, the application of the different criteria in complex turbulent flows has been generally with some non-zero threshold. The non-zero threshold certainly introduces some arbitrariness into vortex core identification through the choice of its value. Nevertheless, a non-zero threshold is quite appealing since the interest is in identifying intense vortical structures. For example, figure 7 shows the vortex cores as identified by the
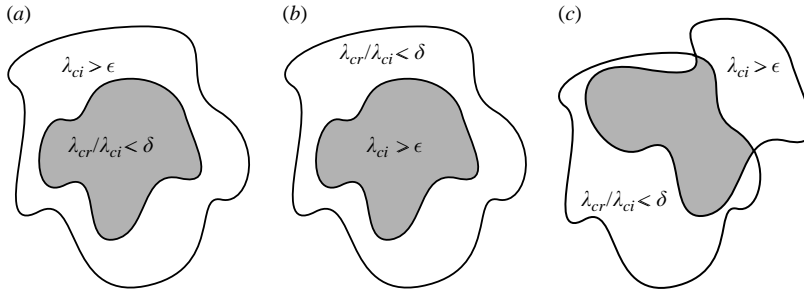
FIGURE 8. A schematic representation of vortex core requirement under different possible scenarios.

$\Delta > 0$ or $\lambda_{ci} > 0$ and $\lambda_2 < 0$ criteria applied to a box of isotropic turbulence computed on a $(256)^3$ grid at a Taylor microscale Reynolds number of 164 (Langford & Moser 1999). The vortex cores as extracted by the two different criteria with zero threshold are qualitatively similar and tend to be volume filling. The worm-like intense vortical structures that are characteristic of isotropic turbulence can be extracted only with an appropriate non-zero threshold (as will be shown in § 5.3.1). The non-zero λ_{ci} threshold has a clear physical interpretation in terms of rate of rotation of material points in the vortex core and can be judiciously chosen based on the relevant time scales of the problem at hand. Threshold values for the other criteria play a similar role, although the precise physical interpretation may be less clear. It may be noted that non-local schemes can be formulated where a threshold need not be explicitly imposed, but can result from imposing a criterion on the spatial variation of some non-local parameter (for example see Tanahashi, Miyauchi & Ikeda 1997, who consider the variance of azimuthal velocity).

Clearly the Q, Δ, λ_{ci}, and λ_2 criteria are not identical and as a result some differences do exist between their respective vortex cores. The identified vortex geometry satisfies the requirements of the identification scheme used, and these requirements are different for the different schemes. Nevertheless, it has been observed in several turbulent flows (for example see Zhou *et al.* 1999; Dubief & Delcayre 2000) that the vortex core structures extracted by the different criteria using non-zero thresholds are quite similar. Our experience with different turbulent flows indicates that the intense vortical regions in these flows share a special property (captured using $\lambda_{cr}/\lambda_{ci}$). In these flows, for extracting similar vortex cores of sufficient intensity, the key is the appropriate choice of the threshold. In this section we formulate the notion of the equivalence of thresholds and the conditions needed for its applicability. With thresholds of 'equivalent magnitude' for the different criteria, the resulting vortex cores are quite similar for all practical purposes of kinematic and dynamic interpretation.

5.1. *Equivalent threshold*

Here we consider the following problem: given the threshold conditions

$$\lambda_{ci} \geqslant (\lambda_{ci})_{th} = \epsilon \qquad \text{and} \qquad (\lambda_{cr}/\lambda_{ci}) \leqslant (\lambda_{cr}/\lambda_{ci})_{th} = \delta, \qquad (5.1)$$

what are the corresponding 'equivalent' thresholds for Q, Δ, and λ_2? This equivalence is in the sense of extracting similar vortex regions. The above threshold conditions for λ_{ci} and $\lambda_{cr}/\lambda_{ci}$ are appealing since they have precise interpretations in terms of local measures of the rate of rotation and spiralling compactness inside the vortex core. As illustrated in figure 8, the interplay between the two thresholds can be complicated.
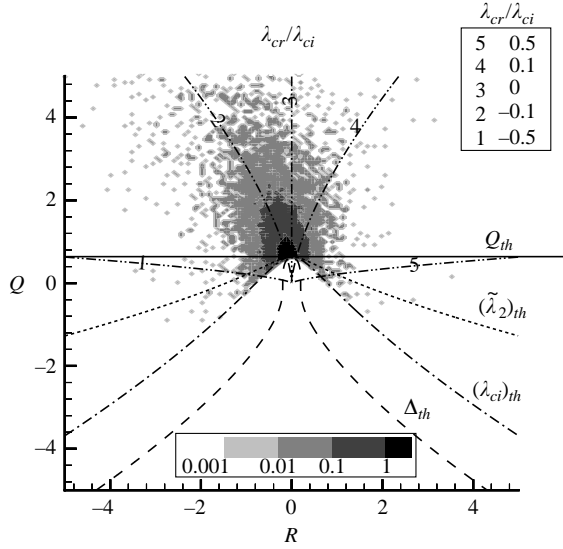
FIGURE 9. Contour lines (in the Q, R-plane) of $(\lambda_{ci})_{th} = \epsilon = 0.8$ (– · – · –) with the corresponding Q_{th} (———), Δ_{th} (– – –), and $\tilde{\lambda}_{2th}$ (· · · · · ·), as defined in equation (5.2). Also plotted are the contour lines of $\lambda_{cr}/\lambda_{ci}$ (–· · · · –) and the shaded contours that represent the joint probability density function between Q and R for the worms of isotropic turbulence identified by $(\lambda_{ci})_{th} = 0.8$ (refer to §5.3.1).

For example, the region identified by $\lambda_{cr}/\lambda_{ci} \leqslant \delta$ can be completely embedded within the region identified by $\lambda_{ci} \geqslant \epsilon$ (see frame *a*), in which case the vortex core is simply identified by the former condition with the value of λ_{ci} varying along its boundary. Frame (*b*) illustrates the converse scenario where $\lambda_{ci} \geqslant \epsilon$ subsumes the $\lambda_{cr}/\lambda_{ci} \leqslant \delta$ condition. A more complex scenario is depicted in frame (*c*).

It is clear from figure 2 that no single threshold value for Q, Δ, or $\tilde{\lambda}_2$ will precisely replicate the vortex core extracted by equation (5.1). Similarly, the converse is also true: no single values of λ_{ci} and $\lambda_{cr}/\lambda_{ci}$ can precisely capture the vortex core obtained from some threshold for Q, Δ or $\tilde{\lambda}_2$. (This can also be inferred from the equations relating these criteria.) Here, as an alternative, we seek simple equivalent threshold conditions that extract essentially similar vortex core structures when applied to realistic complex flows of interest. Our proposal is based on the following observation: inside the intense vortical structures of most turbulent flows, the swirling motion dominates and the ratio $|\lambda_{cr}/\lambda_{ci}|$ takes small values. For incompressible flows the limit $\lambda_{cr}/\lambda_{ci} \to 0$ corresponds to two-dimensional motion in the vortex plane, thereby indicating that the local motion in the intense structures is essentially planar with limited radial motion. This observation confirms to the intuitive notion of an intense swirling region. Figure 9 shows the joint probability density between Q and R for worms in isotropic turbulence along with contour lines of $\lambda_{cr}/\lambda_{ci}$. It is clear that the most likely values of $|\lambda_{cr}/\lambda_{ci}|$ are quite small and this is typical of most other turbulent flows as well. Based on the above observation, a simple proposal is

$$Q \geqslant Q_{th} = \epsilon^2, \tag{5.2a}$$

$$\Delta \geqslant \Delta_{th} = \tfrac{1}{27}\epsilon^6, \tag{5.2b}$$

$$\lambda_2 \leqslant (\lambda_2)_{th} = (\tilde{\lambda}_2)_{th} = -\epsilon^2. \tag{5.2c}$$

The above thresholds become exact for $\lambda_{cr}/\lambda_{ci} = 0$. Note that λ_2 and $\tilde{\lambda}_2$ are equal in this limit. Figure 9 shows the contour line of $\lambda_{ci} = \epsilon$ along with the corresponding lines of $Q = Q_{th}$, $\Delta = \Delta_{th}$, and $\tilde{\lambda}_2 = (\tilde{\lambda}_2)_{th}$, with the threshold values of Q, Δ, and $\tilde{\lambda}_2$ defined by equation (5.2). The different criteria are in agreement at the apex (at $\lambda_{cr}/\lambda_{ci} = 0$). It can be readily seen that the vortex core extracted by the Q criterion as defined above will be the smallest structure and the vortex cores extracted by the λ_{ci} and Δ criteria will be progressively larger. No such definitive statement can be made about the λ_2 criterion as it cannot be uniquely determined from Q and R. As a proxy in figure 9 we have plotted the contour line of $\tilde{\lambda}_2 = (\tilde{\lambda}_2)_{th}$, which extracts a vortex core that is intermediate in size between those extracted by the Q and λ_{ci} criteria. The equivalent threshold definition given in equation (5.2) is clearly non-optimal. More elaborate definitions of equivalent thresholds can be proposed in replacement of equation (5.2) and these definitions can be designed to optimize, say, the degree of overlap between the extracted vortex cores. Such optimization will be flow dependent and hence will not be pursued here. More importantly, we will see that in turbulent flows that we investigate (see § 5.3), the thresholds as defined above yield vortex core structures that are nearly identical for purposes of kinematic and dynamic interpretation. It is important to note that this simple proposal is valid for $\lambda_{cr}/\lambda_{ci} \to 0$ and significant differences can emerge as the inverse spiralling compactness becomes non-zero.

5.2. Burgers' vortex revisited

Here we re-examine the Burgers' vortex in the context of a non-zero threshold for the different criteria. For any given threshold, say $\lambda_{ci} = \epsilon$, the corresponding precise thresholds for the Q, Δ, and λ_2 criteria can be found that will extract identical vortex cores for this problem. For the Q and Δ criteria, the corresponding precise thresholds depend on the axisymmetric strain rate ξ as well

$$Q_{th} = \epsilon^2 - 3\xi^2 \qquad \text{and} \qquad \Delta_{th} = \frac{1}{27}\epsilon^2\xi^4\left(9 + \frac{\epsilon^2}{\xi^2}\right)^2. \tag{5.3}$$

For the λ_2 criterion, the precise threshold that extracts an identical vortex core depends on both ξ and Re. Consider now a complex flow field composed of a superposition of Burgers' vortices with varying strain rate ξ and Reynolds number Re. Since the thresholds depend on the strain rate (and Reynolds number in the case of λ_2), given a threshold $\lambda_{ci} = \epsilon$, it is not possible to identify a unique threshold for the other criteria that will extract vortices identical to that from $\lambda_{ci} = \epsilon$. This will be the likely scenario in a complex turbulent flow. The best one can hope for is to identify equivalent thresholds that will optimize the overlap of the vortex cores identified by the different criteria. For an assembly of Burgers' vortices such an optimization can be performed in terms of the statistical properties of the assembly.

Here we apply the simple equivalent thresholds presented in equation (5.2) to the case of a Burgers' vortex to evaluate its effectiveness. Figure 10 shows the Burgers' vortex core radius extracted by the different criteria as a function of ϵ^2/Re^2. At $Re = 10$, the differences in the vortex core radii are significant. As expected, the vortex core radii extracted by the different criteria in decreasing order are: Δ, λ_{ci}, $\tilde{\lambda}_2$, and Q. The radius extracted using the λ_2 criterion does not follow such a trend, but it remains close to the radii obtained using Q and $\tilde{\lambda}_2$. The above behaviour of the different criteria remains the same with increasing Reynolds number, but the differences become increasingly insignificant. At $Re = 30$, the differences between the vortex core radii extracted by the different criteria are almost negligible. This is expected because $\lambda_{cr}/\lambda_{ci} \sim Re^{-1}$ (refer to the argument in § 4.4.1). Thus, it is clear
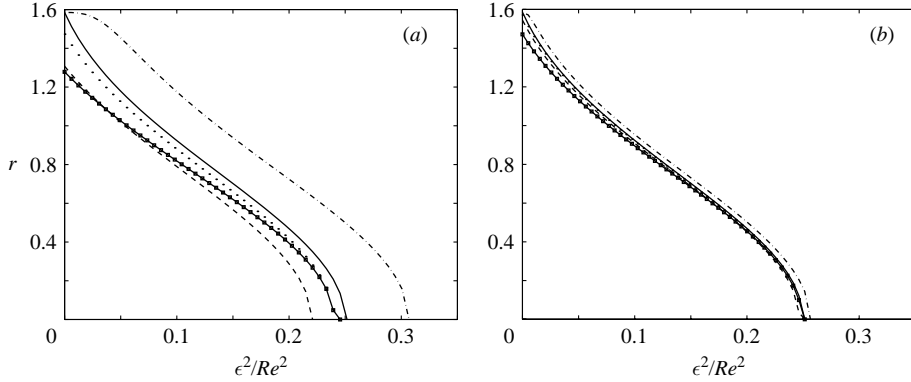
FIGURE 10. Burgers' vortex core radius as a function of threshold used for: (*a*) $Re = 10$; (*b*) $Re = 30$. The different lines represent: Δ_{th} (– · – · –), $(\lambda_{ci})^2_{th}$ (———), $\tilde{\lambda}_{2th}$ (· · · · · ·), λ_2 (–■–■–), and Q_{th} (– – –).

that with increasing intensity of the vortex, the differences between the various criteria diminish.

5.3. *Application to turbulent flows*

Three canonical cases of turbulent flows are studied: forced isotropic turbulence, wake flow behind a sphere, and channel flow. It is seen that using the proposal for equivalent thresholds all the criteria result in almost identical vortical structures. In this section we look at the case of isotropic turbulence. The results for the other flows follow the same trend (refer to Chakraborty, Balachandar & Adrian 2004).

5.3.1. *Forced isotropic turbulence*

We use 256^3 DNS data (Langford & Moser 1999) of incompressible forced isotropic turbulence at Reynolds number (based on Taylor microscale) $Re_\lambda = 164$. We are interested in identifying the coherent vortical structures in this flow. The familiar vortex 'worms' of isotropic turbulence are intense vortical structures and hence to capture these worms we impose a high rate of rotation requirement by selecting $(\lambda_{ci})_{th}\eta/u_\eta = 0.8$. Here η and u_η are the Kolmogorov length and velocity scales respectively. Based on the above threshold for λ_{ci}, we determine the equivalent thresholds for the other criteria using the proposal of equation (5.2). The vortex worms are regions of intense swirling and the values of $|\lambda_{cr}/\lambda_{ci}|$ inside them are very small (refer to figure 9). Hence we expect the equivalent-threshold proposal to result in similar looking vortical structures. Indeed, this expectation is confirmed in figure 11, which depicts the vortex cores identified by the different criteria. In spite of the simplicity of the equivalence of the different thresholds, the resulting structures for the λ_{ci}, Q, λ_2, and $\tilde{\lambda}_2$ criteria are strikingly similar for the purposes of kinematic and dynamic interpretation.

The only difference seems to be the Δ criterion, which appears to be noisy in certain regions of the flow (highlighted in figure 11*c*). We note that this behaviour of the Δ criterion is in agreement with that observed by Jeong & Hussain (1995). The values of $\lambda_{cr}/\lambda_{ci}$ at these highlighted places of noisy vortex core were found to be quite high. This results in a high value of Δ even though local swirling of the flow, as measured by λ_{ci}, is low. These regions do not qualify as vortex core for both low values of λ_{ci} and large values of $\lambda_{cr}/\lambda_{ci}$. Nevertheless, the Δ criterion owing to its definition

(a)

(b)

(c)

(d)

(e)

(f)

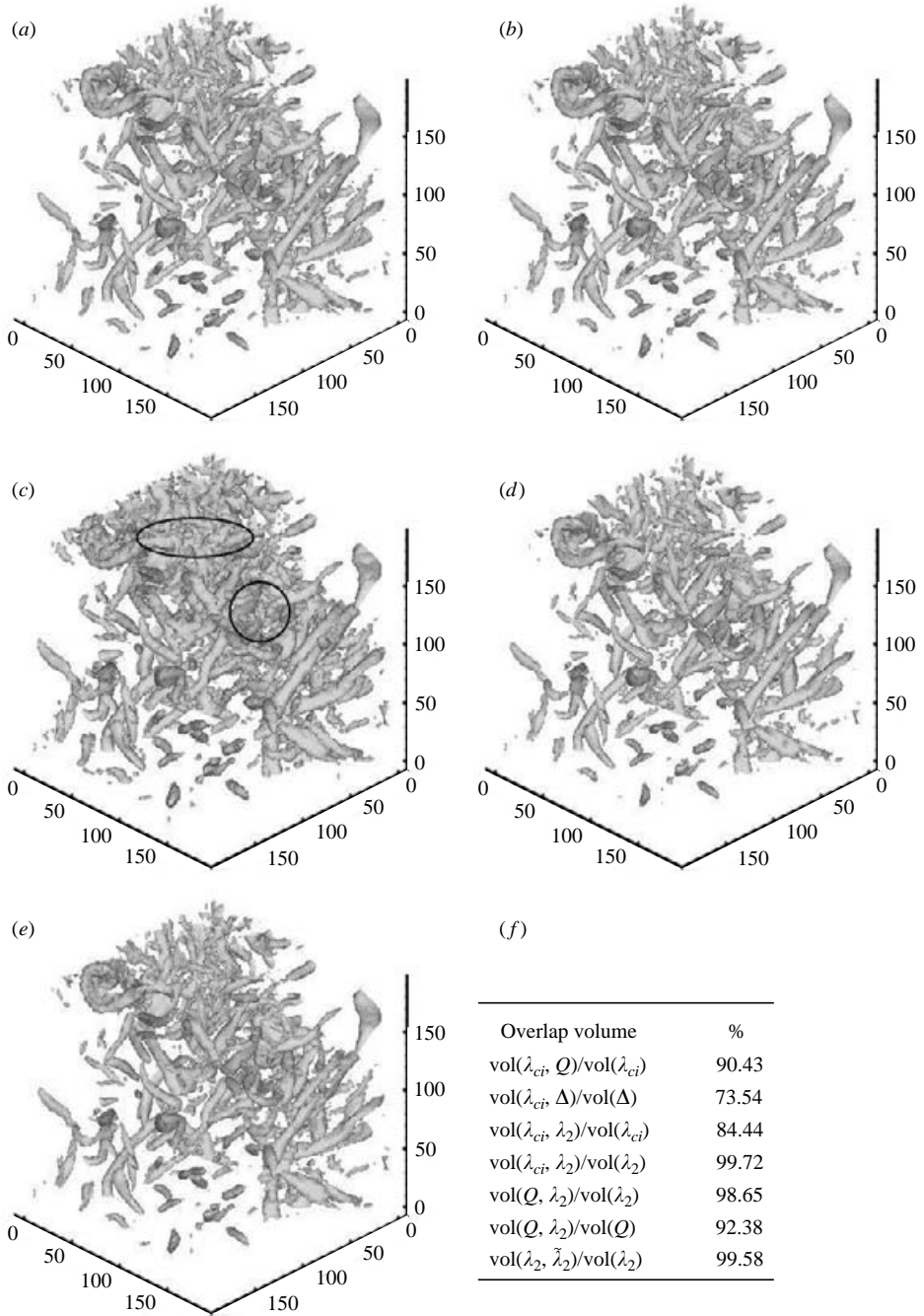| Overlap volume	%
$\mathrm{vol}(\lambda_{ci}, Q)/\mathrm{vol}(\lambda_{ci})$	90.43
$\mathrm{vol}(\lambda_{ci}, \Delta)/\mathrm{vol}(\Delta)$	73.54
$\mathrm{vol}(\lambda_{ci}, \lambda_2)/\mathrm{vol}(\lambda_{ci})$	84.44
$\mathrm{vol}(\lambda_{ci}, \lambda_2)/\mathrm{vol}(\lambda_2)$	99.72
$\mathrm{vol}(Q, \lambda_2)/\mathrm{vol}(\lambda_2)$	98.65
$\mathrm{vol}(Q, \lambda_2)/\mathrm{vol}(Q)$	92.38
$\mathrm{vol}(\lambda_2, \tilde{\lambda}_2)/\mathrm{vol}(\lambda_2)$	99.58

FIGURE 11. Vortex worms in isotropic turbulence. For the sake of clarity $(1/4)^3$ of the volume of the entire simulation box is shown. The different non-dimensional thresholds are computed using equation (5.2) for $(\lambda_{ci})_{th} = 0.8$: (a) λ_{ci}; (b) Q; (c) Δ; (d) λ_2; (e) $\tilde{\lambda}_2$. Frame (f) shows the quantitative comparison of the overlapping volume measure for the different criteria.

(equation (4.2)), identifies them as vortex core. If the Δ definition is augmented by stripping off regions with high $\lambda_{cr}/\lambda_{ci}$, these noisy regions disappear.

The visualization of the vortex isosurfaces involves interpolating the vortex identification parameter between the computational grid points. These quantities are computed using powers of ∇v components (for example, computation of Δ involves sixth power), and they are accurate at the grid points. Nevertheless, if spectral interpolation is used to visualize the isosurfaces, the interpolated region may be corrupted by aliasing effects.

6. Conclusion

The presence of viscosity in real fluids results in continuity in the kinematic features of the flow field. This allows the use of local behaviour to make a reasonable estimate of some non-local features of the flow in space and time. We have addressed the problem of identifying the vortex cores using local schemes. This work is not restricted exclusively to fluid flows, but can be applied to any smooth three-dimensional vector fields.

A proposal for the features in a vortex core was made using the ideas of swirling rate and orbital compactness. Local flow kinematic parameters were identified to provide a measure of the swirling rate (λ_{ci}) and inverse spiralling compactness ($\lambda_{cr}/\lambda_{ci}$), which have a precise mathematical foundation and unambiguous physical interpretation.

The inter-relationships between the different local criteria were explored. Closed-form relations were obtained for relating the local kinematic parameters λ_{ci} and $\lambda_{cr}/\lambda_{ci}$, with Q and Δ. Such a relation with λ_2 is not possible except for the special case of orthonormal eigenvectors of ∇v. This special case was used to approximate the behaviour of the λ_2 criterion and was called $\tilde{\lambda}_2$. A generic characterization of the region identified by $\lambda_2 < 0$ was made by analysing all the possible configurations of ∇v. These inter-relationships provide a new interpretation of the various criteria in terms of the local flow kinematics. Characterization of the different criteria was done for both zero and the commonly employed non-zero thresholds. Based on the observation that a region of intense swirling is approximately locally two-dimensional with limited radial motion, a simple proposal for the thresholds for Q, Δ, and λ_2 was proposed based on the threshold for λ_{ci}. It was observed that in the intense swirling regions (for example a Burgers' vortex at high Re or vortical structures in turbulent flows), the vortex structures educed using these thresholds were identical for the purposes of kinematic and dynamic interpretation.

The case of a swirling jet, where the different criteria result in conflicting identification of vortical regions, was explained on the basis of inverse spiralling compactness ($\lambda_{cr}/\lambda_{ci}$) parameter values. It was seen that using a non-zero threshold with the Δ criterion can be quite misleading. Nonetheless, for most of the cases of practical interest, additionally using an appropriate threshold for $\lambda_{cr}/\lambda_{ci}$ will result in similar vortical structures. To be useful as a qualitative and a quantitative tool for understanding the fundamental processes in turbulence, it is imperative that these thresholds have a clear interpretation. In this sense, the present proposal has an advantage since both λ_{ci} and the ratio $\lambda_{cr}/\lambda_{ci}$ have a simple and precise interpretation of the local flow kinematics (for both zero and non-zero threshold).

Appendix. Bounds on the eigen-spectrum

It was noted that λ_2 cannot be expressed solely in terms of the eigenvalues of ∇v. Here we explore the possibility of specifying bounds on the eigenvalues of $S^2 + \Omega^2$. The idea is to obtain a range of variation of λ_2 when the eigenvalues of ∇v are known. We restrict our analysis to the case when ∇v has complex eigenvalues.

A.1. *Bromwich bounds*

It can be shown that

$$S^2 + \Omega^2 = \text{sym}(\nabla v^2). \tag{A 1}$$

From the trace equality condition (i.e. $\text{tr}[\text{sym}(\nabla v^2)] = \text{tr}[S^2 + \Omega^2]$), we obtain

$$\lambda_1 + \lambda_2 + \lambda_3 = 2\lambda_{ci}^2 \left(3\left(\frac{\lambda_{cr}}{\lambda_{ci}}\right)^2 - 1 \right). \tag{A 2}$$

Using Bromwich bounds (Mirsky 1963) for the real part of eigenvalues of ∇v^2, we obtain

$$\lambda_1 \geqslant 4\lambda_{cr}^2, \tag{A 3a}$$
$$\lambda_3 \leqslant \lambda_{cr}^2 - \lambda_{ci}^2. \tag{A 3b}$$

Combining equations (A 2) and (A 3), we obtain the following inequalities:

$$\lambda_2 + \lambda_3 \leqslant 2\lambda_{ci}^2 \left(\left(\frac{\lambda_{cr}}{\lambda_{ci}}\right)^2 - 1 \right), \tag{A 4a}$$

$$\lambda_1 + \lambda_2 \geqslant \lambda_{ci}^2 \left(5\left(\frac{\lambda_{cr}}{\lambda_{ci}}\right)^2 - 1 \right). \tag{A 4b}$$

Using Bromwich bounds for ∇v defined in equation (4.4), we obtain

$$\lambda_{ci} \leqslant a, \tag{A 5a}$$
$$-\frac{1}{2} \leqslant \lambda_{cr} \leqslant \frac{1}{2}\left(1 - \frac{\xi}{2}\right). \tag{A 5b}$$

A.2. *Eigenvalues of sums of Hermitian matrices*

Let the principal strain rates be denoted by $(\sigma_1, \sigma_2, \sigma_3)$, where $\sigma_1^2 \geqslant \sigma_2^2 \geqslant \sigma_3^2$, and the vorticity magnitude be denoted by ω (then the eigenvalues of Ω are $(0, \pm i\omega/2)$). Using the results from Horn (1962), we obtain

$$\left.\begin{array}{r}\sigma_1^2 - \omega^2/4\\ \sigma_3^2\end{array}\right\} \leqslant \lambda_1 \leqslant \sigma_1^2, \tag{A 6a}$$

$$\sigma_2^2 - \omega^2/4 \leqslant \lambda_2 \leqslant \left\{\begin{array}{l}\sigma_1^2 - \omega^2/4\\ \sigma_2^2\end{array}\right., \tag{A 6b}$$

$$\sigma_3^2 - \omega^2/4 \leqslant \lambda_3 \leqslant \left\{\begin{array}{l}\sigma_2^2 - \omega^2/4\\ \sigma_3^2\end{array}\right.. \tag{A 6c}$$

For $\lambda_2 \leqslant 0$, equation (A 6b) becomes

$$\sigma_2^2 - \frac{\omega^2}{4} \leqslant \lambda_2 \leqslant \sigma_1^2 - \frac{\omega^2}{4}. \tag{A 7}$$

Applying the bounds for λ_2 (equation (A 7)) for the case of ∇v of equation (4.4), as well as for the case when $-1 \leqslant \xi \leqslant 0$, we obtain

$$\left(1 - \frac{|\xi|}{2}\right)^2 - \frac{\omega^2}{4} \leqslant \lambda_2 \leqslant 1 - \frac{\omega^2}{4}. \tag{A 8}$$

Note that the above equation assumes that ∇v has the form of equation (4.4), i.e. ignores the scaling factor. Now we show an example of using equation (A 8). Tanahashi, Iwase & Miyauchi (2001) find the strain rate eigenvalues at the centre of the fine-scale eddies in turbulent mixing layers to have the ratio $-5 : 1 : 4$. This implies $\xi = -2/5$ and hence, at the centre of these fine-scale eddies, the values of λ_2 are bounded by (using equation (A 8))

$$\frac{16}{25} - \frac{\omega^2}{4} \leqslant \lambda_2 \leqslant 1 - \frac{\omega^2}{4}. \tag{A 9}$$

REFERENCES

ADRIAN, R. J., MEINHART, C. D. & TOMKINS, C. D. 2000 Vortex organization in the outer region of the turbulent boundary layer. *J. Fluid Mech.* **422**, 1–54.

BERDAHL, C. & THOMPSON, D. 1993 Eduction of swirling structure using the velocity gradient tensor. *AIAA J.* **31**, 97–103.

BROOK, J. W. & HANRATTY, T. J. 1993 Origin of turbulence-producing eddies in a channel flow. *Phys. Fluids* A **5**, 1011–1022.

BURGERS, J. M. 1948 A mathematical model illustrating the theory of turbulence. *Adv. Appl. Mech.* **1**, 171–199.

CANTWELL, B. J. 1981 Organized motion in turbulent flow. *Annu. Rev. Fluid Mech.* **13**, 457–515.

CHAKRABORTY, P., BALACHANDAR, S. & ADRIAN, R. J. 2004 Local vortex identification criteria: inter-relationships and a unified outlook. In *IUTAM Symposium on Elementary Vortices and Coherent Structures: Significance in Turbulence Dynamics* (ed. S. Kida, Y. Yamada & S. Yoden).

CHONG, M. S., PERRY, A. E. & CANTWELL, B. J. 1990 A general classification of three-dimensional flow fields. *Phys. Fluids* A **2**, 765–777.

CUCITORE, R., QUADRIO, M. & BARON, A. 1999 On the effectiveness and limitations of local criteria for the identification of a vortex. *Eur. J. Mech.* B/*Fluids* **18**, 261–282.

DUBIEF, Y. & DELCAYRE, F. 2000 On coherent-vortex identification in turbulence. *J. Turbulence* **1**, 1–22.

HEAD, M. R. & BANDYOPADHYAY, P. 1981 New aspects of turbulent boundary layer structure. *J. Fluid Mech.* **107**, 287–338.

HORIUTI, K. 2001 A classification method for vortex sheet and tube structures in turbulent flows. *Phys. Fluids* **13**, 3756–3774.

HORN, A. 1962 Eigenvalues of sums of hermitian matrices. *Pacific J. Maths* **12**, 225–241.

HUNT, J. C. R., WRAY, A. A. & MOIN, P. 1988 Eddies, stream, and convergence zones in turbulent flows. *Center for Turbulence Research Report* CTR-S88, pp. 193–208.

HUSSAIN, A. K. M. F. 1986 Coherent structures and turbulence. *J. Fluid Mech.* **173**, 303–356.

JEONG, J. & HUSSAIN, F. 1995 On the identification of a vortex. *J. Fluid Mech.* **285**, 69–94.

JIMÉNEZ, J., WRAY, A. A., SAFFMAN, P. G. & ROGALLO, R. S. 1993 The structure of intense vorticity in isotropic turbulence. *J. Fluid Mech.* **255**, 65–90.

KÜCHERMANN, D. 1965 Report on the IUTAM symposium on concentrated vortex motion in fluids. *J. Fluid Mech.* **21**, 1–20.

LANGFORD, J. A. & MOSER, R. D. 1999 Optimal LES formulations for isotropic turbulence. *J. Fluid Mech.* **398**, 321–346.

LUGT, H. J. 1979 The dilemma of defining a vortex. In *Recent developments in Theoretical and Experimental Fluid Mechanics* (ed. U. Müller, K. Roesner & B. Schimdt), pp. 309–321. Springer.

MARUSIC, I. 2001 On the role of large-scale structures in wall turbulence. *Phys. Fluids* **13**, 735–743.

MIRSKY, L. 1963 *An Introduction to Linear Algebra*. Oxford University Press.

MOORE, D. W. & SAFFMAN, P. G. 1972 The motion of a vortex filament with axial flow. *Phil. Trans. R. Soc. Lond.* A **338**, 403–429.

PERRY, A. E. & MARUSIC, I. 1995 A wall-wake model for the turbulence structure of boundary layers part 1. extension of the attached eddy hypothesis. *J. Fluid Mech.* **298**, 361–388.

PULLIN, D. I. & SAFFMAN, P. G. 1998 Vortex dynamics in turbulence. *Annu. Rev. Fluid Mech.* **30**, 31–51.

ROBINSON, S. K. 1991 Coherent motion in the turbulent boundary layer. *Annu. Rev. Fluid Mech.* **23**, 601–639.

ROGERS, M. M. & MOSER, R. D. 1994 Direct simulation of a self-similar turbulent mixing layer. *Phys. Fluids* **6**, 903–923.

SAFFMAN, P. G. 1992 *Vortex Dynamics*. Cambridge University Press.

SHTERN, V. & HUSSAIN, F. 1993 Hysteresis in a swirling jet as a model tornado. *Phys. Fluids* A **5**, 2183–2195.

SMITH, C. R., WALKER, J. D. A., HAIDARI, A. H. & SOBRUN, U. 1991 On the dynamics of near-wall turbulence. *Phil. Trans. R. Soc. Lond.* A **336**, 131–175.

TANAHASHI, M., IWASE, S. & MIYAUCHI, T. 2001 Appearance and alignment with strain rate of coherent fine scale eddies in turbulent mixing layer. *J. Turbulence* **2** (6), 1–17.

TANAHASHI, M., MIYAUCHI, T. & IKEDA, J. 1997 Identification of coherent fine scale structure in turbulence. In *IUTAM Symposium on Simulation and Identification of Organized Structures in Flows* (ed. J. Sørensen, E. Hopfinger & N. Aubry), pp. 131–140. Kluwer.

TANAKA, M. & KIDA, S. 1993 Characterization of vortex tubes and sheets. *Phys. Fluids* A **5**, 2079–2082.

ZHOU, J., ADRIAN, R. J., BALACHANDAR, S. & KENDALL, T. M. 1999 Mechanisms for generating coherent packets of hairpin vortices. *J. Fluid Mech.* **387**, 353–396.